Catena 110 (2013) 59–69

Contents lists available at SciVerse ScienceDirect

Catena

journal homepage: www.elsevier.com/locate/catena

Mangrove vegetation changes on Holocene terraces of the Doce River, southeastern Brazil

Marlon C. França [a,b,c], Marcelo C.L. Cohen [a,*], Luiz C.R. Pessenda [d], Dilce F. Rossetti [e], Flávio L. Lorente [d], Antônio Álvaro Buso Junior [d], José T.F. Guimarães [a], Yuri Friaes [a], Kita Macario [f]

[a] Post-Graduate Program of Geology and Geochemistry, Laboratory of Coastal Dynamics, Federal University of Pará, Av. Perimentral 2651, Terra Firme, CEP: 66077-530 Belém, PA, Brazil
[b] Federal Institute of Pará, Av. Almirante Barroso, 1155, Marco, CEP: 66090-020 Belém, PA, Brazil
[c] Climate System Research Center, Department of Geosciences, University of Massachusetts, Amherst, MA 01003, USA
[d] University of São Paulo, ^{14}C Laboratory, Avenida Centenário 303, CEP: 13400-000 Piracicaba, SP, Brazil
[e] National Space Research Institute (INPE), Rua dos Astronautas 1758-CP 515, CEP: 12245-970 São José dos Campos, SP, Brazil
[f] LAC-UFF AMS Laboratory-Fluminense Federal University, Physics Department, Niteroi, Rio de Janeiro, Brazil

A R T I C L E I N F O

Article history:
Received 9 January 2013
Received in revised form 2 April 2013
Accepted 4 June 2013
Available online xxxx

Keywords:
Facies analyses
Holocene
Mangrove
Palynology
Sea-level
Stable isotopes

A B S T R A C T

High-resolution sedimentological, geochemical and pollen analysis on sediment core from the coastal plain of the Doce River, southeastern Brazil, revealed changes in the depositional system and vegetation caused by combined action of oscillations in relative sea-level (RSL) and sedimentary supply during the Holocene. Two main phases were discerned using sedimentary features, $\delta^{13}C$, $\delta^{15}N$, total organic carbon (TOC), total nitrogen (N), C/N and cluster analysis of pollen data, temporally synchronized with radiocarbon age dating. The data indicates the presence of a lagoon system surrounded by a tidal plain colonized by mangroves and its sedimentary organic matter sourced from C_4 plants between ~8050 and ~7115 cal yr BP. However, during the mid- and late-Holocene the mangroves shrank and freshwater vegetation expanded (C_3 plants), probably, due to a marine regression. During this phase, the development of a lacustrine environment was followed by the colonization of herbs, trees and shrubs. The continuous sediment infilling into the lake allowed the expansion of a herbaceous plain as seen today. This geomorphologic and vegetation evolution is in agreement with the mid-Holocene RSL maximum above present RSL and subsequent fall to the present time.

1. Introduction

Several studies have presented coastal environmental shifts in response to Holocene sea-level changes (Behling et al., 2001, 2004; Blasco et al., 1996; Cohen et al., 2005a,b, 2012; Ellison, 2005; Engelhart et al., 2007; Fujimoto et al., 1996; Guimarães et al., 2012, 2013; Horton et al., 2005; Monacci et al., 2009, 2011; Parkinson et al., 1994; Smith et al., 2012; Woodroffe, 1981; Yulianto et al., 2004, 2005). The effect of relative sea-level (RSL) changes is apparent in coastal environments, where significant geomorphological changes (Giannini et al., 2007) extend to the mangrove dynamics (Behling et al., 2001, 2004; Cohen and Lara, 2003; Cohen et al., 2004, 2005a,b; França et al., 2012; Guimarães et al., 2012; Lara et al., 2002; Smith et al., 2012; Vedel et al., 2006). The expansion or contraction of mangrove areas is dependent on temperature, soil type, salinity, inundation frequency, sediment accretion, tidal and wave energy (Lugo and Snedaker, 1974). Specifically the mangrove has special physiological and morphological adaptations that allow it to grow in intertidal environments (Alongi, 2008; Blasco et al., 1996; Cahoon and Lynch, 1997; Sanders et al., 2012). Thus this ecosystem may be used as an indicator of coastal change and RSL fluctuations (Blasco et al., 1996).

Along the Brazilian coast, mangroves are found from the extreme northern Brazilian coast in the Oiapoque River (04°20′N) to Laguna (28°30′S) in the southern coast (Schaeffer-Novelli et al., 2000). In northern Brazil the mangroves are extremely irregular and jagged, occurring throughout bays and estuaries (Souza-Filho et al., 2006), with meso- and macrotidal ranges (tidal range of 2 to 4 m and 4 to 6 m, respectively). On the southeastern and southern coast, mangroves are restricted to microtidal (tidal range below 2 m) bays, lagoons or estuarine inlets (Schaeffer-Novelli et al., 1990), which are strongly controlled by climate and oceanographic characteristics (Soares et al., 2012).

Some studies have shown post-glacial sea-level rise at the Brazilian littoral (Angulo and Lessa, 1997; Angulo and Suguio, 1995; Angulo et al., 1999, 2006; Bezerra et al., 2003; Bittencourt et al., 1979; Martin et al., 1996, 2003; Suguio et al., 1985), which inundated inland valleys (Cohen et al., 2005a,b; Martin et al., 1996; Scheel-Ybert, 2000; Souza-Filho et al., 2006), causing changes in depositional systems and also in mangrove area (Amaral et al., 2006, 2012; Cohen et al., 2005a,b; Guimarães et al., 2012; Scheel-Ybert, 2000; Smith et al., 2012).

Investigations in northern Brazil utilizing sedimentological, palynological and geochemical data revealed displacement of the

* Corresponding author. Tel./fax: +55 91 3274 3069.
E-mail address: mcohen@ufpa.br (M.C.L. Cohen).

0341-8162/$ – see front matter © 2013 Elsevier B.V. All rights reserved.
http://dx.doi.org/10.1016/j.catena.2013.06.011

mangrove ecosystem during the Holocene. This shift is attributed to climate, river discharge and RSL changes (Behling et al., 2004; Cohen et al., 2005a, 2008, 2009; França et al., 2012; Guimarães at al., 2012; Lara and Cohen, 2009; Smith et al., 2011, 2012). However, in southeastern Brazil, the mangrove dynamics are mainly related to RSL changes (Buso Junior, 2010; Buso Junior et al., in press) and sediment transport (Amaral et al., 2006).

For the southeastern Brazilian coast environmental reconstructions based on inter-proxy analysis are still scarce, and the response of mangrove ecosystems to Holocene sea-level changes remains poorly understood. In this work we present a study about mangrove development on the coastal plain of the Doce river, State of Espírito Santo, southeastern Brazil, during the Holocene, recorded by multiple proxies such as sedimentary features, $\delta^{13}C$ and $\delta^{15}N$, C/N, pollen data and radiocarbon dating.

2. Modern settings

2.1. Study area and geological setting

The study site is located in the coastal plain between two large rivers (Fig. 1), Doce and São Mateus, northern Espírito Santo—Brazil, running along a nearly N–S section between Conceição da Barra and Barra do Riacho (Bittencourt et al., 2007; Suguio et al., 1982). The Holocene sedimentary history in this sector is strongly controlled by RSL changes, fluvial supply and longshore transport. The formation of a barrier island/lagoonal system began about 7000 yr BP (Martin et al., 1996, 2003; Suguio et al., 1982).

The study area is composed of a Miocene age plateau of Barreiras Formation continental deposits, whose surface is slightly sloping to the ocean. The site is characterized by the presence of many wide valleys with flat bottoms, resulting from Quaternary deposition of silty sediments (Martin et al., 1996). The study area is part of a larger area of tectonically stable Precambrian crystalline rocks. Four geomorphological units are recognized in the area: (1) a mountainous province, made up of Precambrian rocks, with a multidirectional rectangular dendritic drainage net; (2) a tableland area composed of Barreiras Formation constituted by sandstones, conglomerates and mudstones attributed mainly to Neogene fluvial and alluvial fan deposits, but possibly including deposits originating from a coastal overlap associated with Neogene marine transgressions (Arai, 2006; Dominguez et al., 2009). The drainage catchment slopes gently down towards the sea; and (3) a coastal plain area, with fluvial, transitional and shallow marine sediments, which were deposited during RSL changes (Martin and Suguio, 1992) and (4) an inner continental shelf area (Asmus et al., 1971).

2.2. Climate

The region is characterized by a warm and humid tropical climate with annual precipitation averaging 1400 mm (Peixoto and Gentry, 1990). Precipitation generally occurs in the summer with a dry fall–winter season, controlled by the position of the Intertropical Convergence Zone (ITCZ) and the position of the South Atlantic Convergence Zone (SACZ) (Carvalho et al., 2004). The area is entirely located within the South Atlantic trade winds belt (NE–E–SE) that is related to a local high-pressure cell and the periodic advance of the Atlantic Polar Front during the autumn and winter, generating SSE winds (Dominguez et al., 1992; Martin et al., 1998). The rainy season occurs between the months of November and January with a drier period between May and September. The average temperature ranges between 20 and 26 °C.

2.3. Vegetation

The region is composed mainly of tropical rainforest, where the most representative plant families are Annonaceae, Fabaceae, Myrtaceae, Sapotaceae, Bignoniaceae, Lauraceae, Hippocrateaceae, Euphorbiaceae, and Apocynaceae (Peixoto and Gentry, 1990). In the sandy coastal plain, vegetation is characterized by palm trees as well as orchids and bromeliads that grow on the trunks and branches of larger trees. *Ipomoea pes-caprae*, *Hancornia speciosa*, *Chrysobalanus icaco*, *Hirtella Americana* and *Cereus fernambucensis* are also found. The coastal plain of the Doce River is characterized by forest pioneering freshwater species such as *Hypolytrum* sp., *Panicum* sp. and also brackish/marine water species such as *Polygala cyparissias*, *Remiria maritima*, *Typha* sp., *Cyperus* sp., *Montrichardia* sp., *Tapirira guianensis* and *Symphonia globulifera*. A mangrove dominated ecosystem is also present, characterized by *Rhizophora mangle*, *Laguncularia racemosa* and *Avicennia germinans*, which are currently restricted to the northern littoral part of the coastal plain (Bernini et al., 2006). Herbaceous vegetation dominates the sampling site, represented by Araceae, Cyperaceae and Poaceae with some trees and shrubs on edge of the plain (Fig. 2).

3. Materials and methods

3.1. Field work and sampling processing

A LANDSAT image acquired on July 2011 was obtained from INPE (National Institute of Space Research, Brazil). A three-color band composition (RGB 543) image was created and processed using the SPRING 3.6.03 image processing system to discriminate geological features. Topographic data were derived from SRTM-90 data, downloaded from USGS Seamless Data Distribution System (http://srtm.usgs.gov/data/obtainingdata.html). Imagem interpretation of elevation data was carried out using software Global Mapper 12.

The fieldwork was carried out in July 2011. The sediment core LI-32 (5.75 m) (S 19° 11′ 56.1″/W 39° 48′ 1.8″) was taken between Holocene sandy ridges (Fig. 1) from a herbaceous plain using a Russian Sampler (Cohen, 2003). It is located approximately 30 km from Doce River and 10 km from the current southeastern wave-dominated coast (Dominguez et al., 2009). The geographical position of the core was determined by GPS (Reference Datum: SAD69).

3.2. Facies description

The core was X-rayed in order to identify internal sedimentary structures. As recorded in Fig. 3, without the radiography of the core, it would not be possible to evidence such structures. Grain size was determined by laser diffraction using a Laser Particle Size SHIMADZU SALD 2101 in the Laboratory of Chemical Oceanography/UFPA. Prior to identification of the grain size, approximately 0.5 g of each sample was immersed in H_2O_2 to remove organic matter and residual sediments were disaggregated by ultrasound (França, 2010). The grain-size scale of Wentworth (1922) was used in this work with sand (2–0.0625 mm), silt (62.5–3.9 μm) and clay fraction (3.9–0.12 μm). Although the equipment presents reading range between 1000 and 0.03 μm, in the studied core sediment fraction higher than 1 mm or lower than 0.12 μm was not recorded. Following the methods of Harper (1984) and Walker (1992), facies analysis included description of color (Munsell Color, 2009), lithology, texture and structure. The sedimentary facies were codified following Miall (1978).

3.3. Palynological analysis

Considering the interpretative significance of pollen data, there often exists two pollen components in sediment—pollen from “local” vegetation (the crown of the hat), and background pollen from “regional” vegetation (the brim of the hat) (Andersen, 1967; Janssen, 1966, 1973; Sugita, 1994). The terms are useful, even though the distinction cannot be drawn sharply: the transition between the crown and brim is gradual, and the sizes of the crown and brim will differ for each pollen taxon (Davis, 2000).

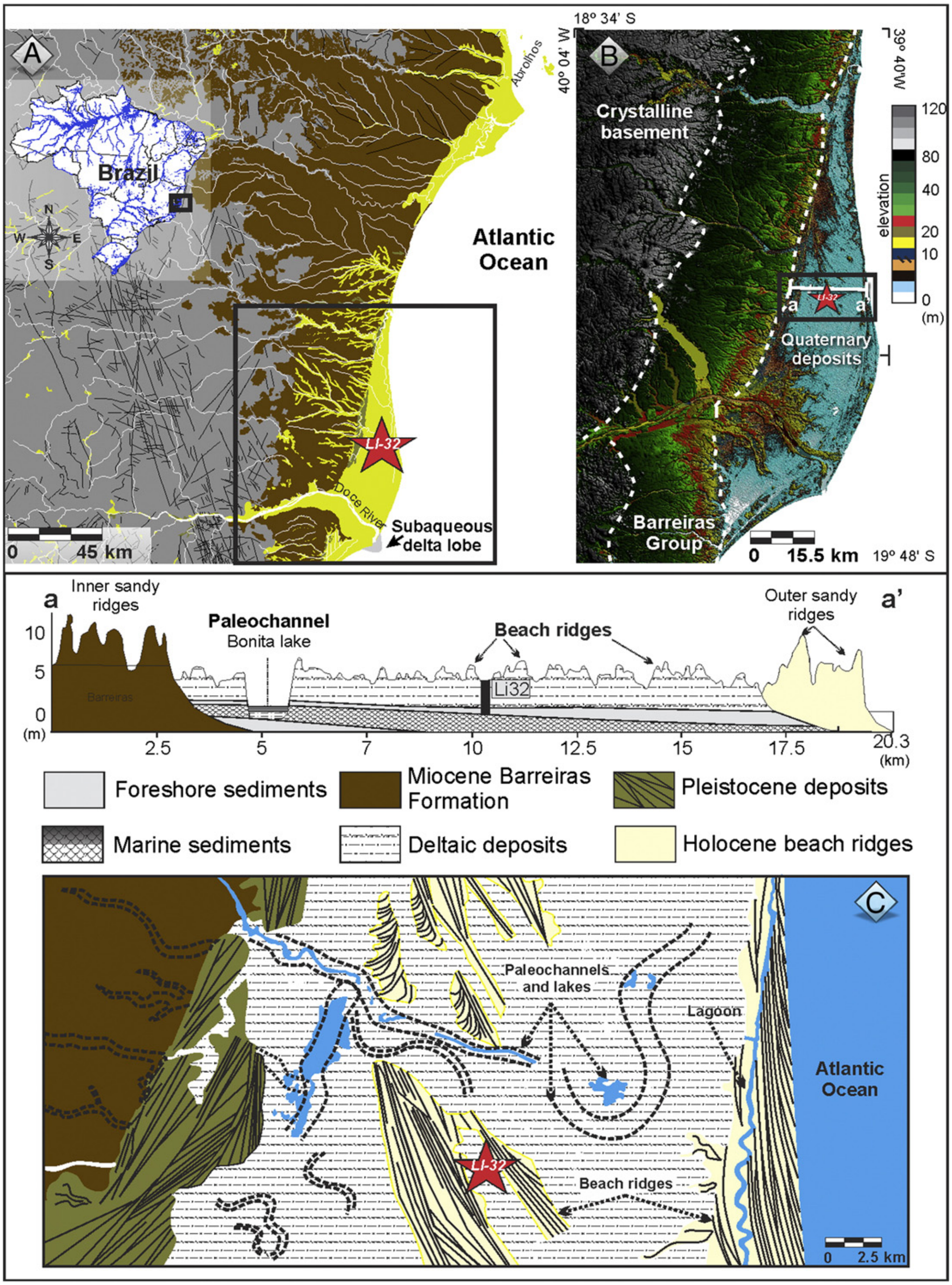

Fig. 1. Location of the study area: a) Miocene Barreiras Formation and coastal plain of the Doce River; b) SRTM-DEM topography of the study site illustrating a large area slightly more depressed on the coastal plain of the Doce River. Note a morphometric profile along the main geological features and morphological units (a–a′); c) paleodrainage networks preserved, with lagoons and lake system originated at the Holocene. Note the presence of Pleistocene deposits. The beach ridges which are related to coastal progradation are also observed.

The pollen records of sediment cores in lakes assume that pollen accumulating in a lake represents the vegetation on all sides of the lake, on the assumption that breezes blow from various directions and the drainage basin area of the lake receive the pollen production. Thus, the strength of the pollen signal from each vegetation is distance-weighted (e.g. Davis, 2000). According to Cohen et al. (2008), pollen profiles from tidal plains present a smaller spatial representativeness of the vegetation than pollen records from lakes. Considering the paleo-lagoon described in this work as a shallow body of water separated from the ocean by barrier islands, the pollen signal in its bottom sediment should reflect the regional paleovegetation, while the pollen preserved in foreshore sediment may represent the pollen transported by rivers and tidal channels to the littoral.

For pollen analysis 1.0 cm^3 samples were taken at 5.0 cm intervals downcore, for a total of 116 samples. All samples were prepared using standard pollen analytical techniques including acetolysis (Faegri and Iversen, 1989). Sample residues were mounted on slides in a glycerin

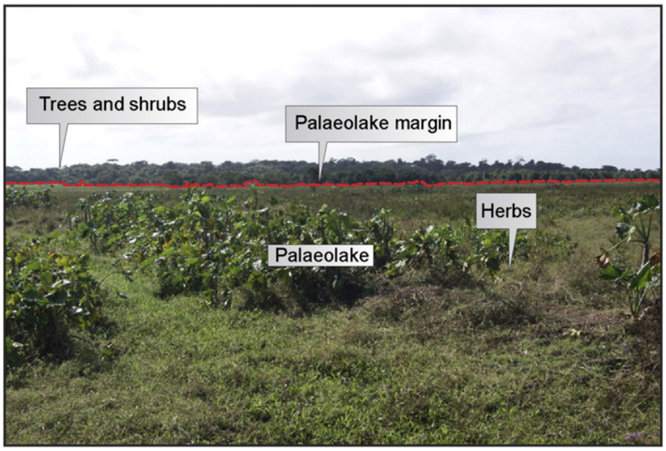

Fig. 2. The sharp contact between arboreal vegetation and herbaceous vegetation indicates the transition zone between paleolake and the edge at the coastal plain of the Doce River. The herbs are the current vegetation which has been developed during the past 3043 cal yr BP on the paleolake.

gelatin medium. Pollen and spores were identified by comparison with reference collections of about 4000 Brazilian forest taxa and various pollen keys (Absy, 1975; Colinvaux et al., 1999; Markgraf and D'Antoni, 1978; Roubik and Moreno, 1991; Salgado-Laboriau, 1973) jointly with the reference collection of the Laboratory of Coastal Dynamics-Federal University of Pará and ^{14}C Laboratory of the Center for Nuclear Energy in Agriculture (CENA/USP) to identify pollen grains and spores. A minimum of 300 pollen grains were counted for each sample. The total pollen sum excludes fern spores, algae, and foraminiferal tests. Pollen and spore data are presented in pollen diagrams as percentages of the total pollen sum. The taxa were grouped according to source: mangrove, tree and shrub, palm, herb and aquatic pollen. The software TILIA and TILIAGRAF were used for calculation and to plot the pollen diagram (Grimm, 1990). CONISS was used for cluster analysis of pollen taxa, permitting the zonation of the pollen diagram (Grimm, 1987).

3.4. Isotopic and chemical analysis

A total of 232 samples (6–50 mg) were collected at 5 cm intervals from the sediment core. Sediments were treated with 4% HCl to eliminate carbonate, washed with distilled water until the pH reached 6, dried at 50 °C, and finally homogenized. These samples were analyzed for total organic carbon and nitrogen, carried out at the Stable Isotope Laboratory of the Center for Nuclear Energy in Agriculture (CENA/USP). The results are expressed as a percentage of dry weight, with analytical precision of 0.09% (TOC) and 0.07% (TN), respectively. The ^{13}C and ^{15}N results are expressed as $\delta^{13}C$ and $\delta^{15}N$ with respect to VPDB standard and atmospheric air, using the following notation:

$$\delta^{13}C(‰) = \left[\left(R_{1\text{sample}}/R_{2\text{standard}}\right)-1\right]\cdot 1000$$

$$\delta^{15}N(‰) = \left[\left(R_{3\text{sample}}/R_{4\text{standard}}\right)-1\right]\cdot 1000$$

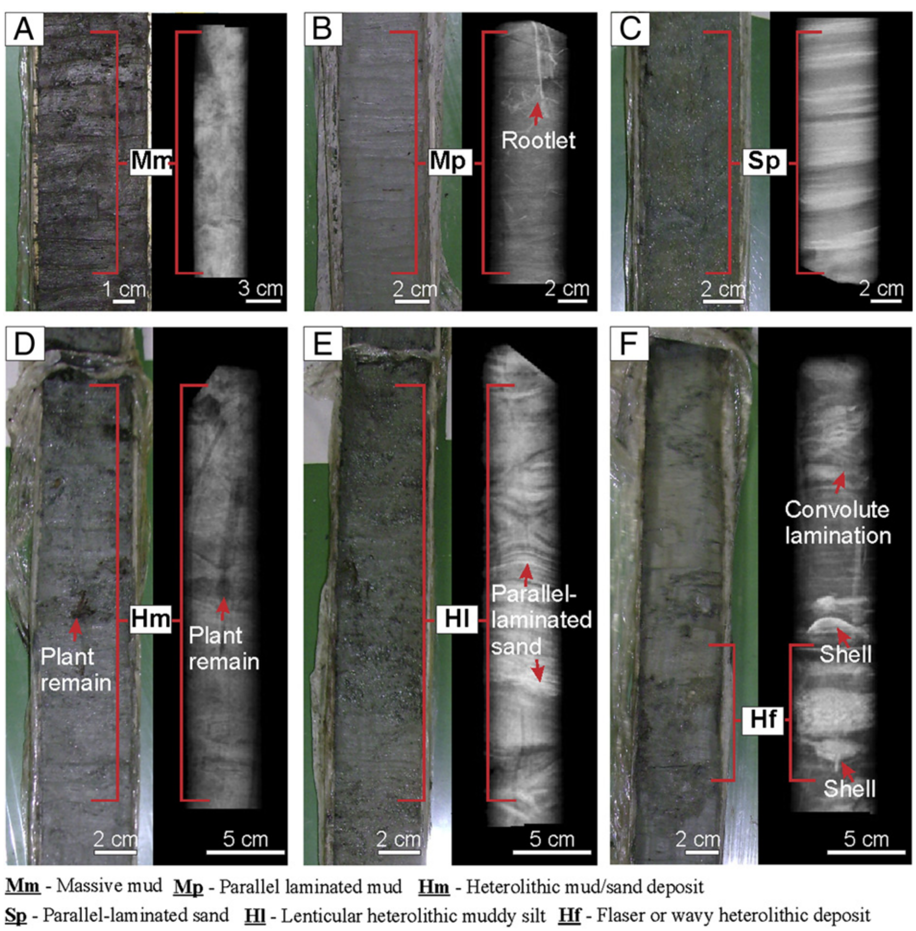

Fig. 3. The X-ray of the core with examples of sedimentary facies of the tidal plain deposits, illustrating: a) massive mud (facies Mm); b) parallel laminated mud (facies Mp), with rootlets and root marks; c) parallel-laminated sand (facies Sp); d) heterolithic mud/sand deposit with plant remains (facies Hm); e) lenticular heterolithic muddy silt with cross lamination (facies Hl); and f) sandy layer, heterolithic mud/sand deposit with convolute lamination and shells (facies Hf).

where $R_{1sample}$ and $R_{2standard}$ are the $^{13}C/^{12}C$ ratio of the sample and standard, and $R_{3sample}$ and $R_{4standard}$ are the $^{15}N/^{14}N$, respectively. Analytical precision is ±0.2‰ (Pessenda et al., 2004).

3.5. Radiocarbon dating

Based on stratigraphic discontinuities that suggest changes in the tidal inundation regime, four bulk samples (10 g each) were selected for radiocarbon analysis. In order to avoid natural contamination by shell fragments, roots, seeds, etc., (e.g. Goh, 2006), the sediment samples were checked and physically cleaned under the stereomicroscope. The organic matter was chemically treated to remove the presence of a younger organic fraction (fulvic and/or humic acids) and to eliminate adsorbed carbonates by placing the samples in 2% HCl at 60 °C for 4 h, followed by a rinse with distilled water to neutralize the pH. The samples were dried at 50 °C. A detailed description of the chemical treatment for sediment samples can be found in Pessenda et al. (2010, 2012). A chronologic framework for the sedimentary sequence was provided by conventional and accelerator mass spectrometer (AMS) radiocarbon dating. Samples were analyzed at the ^{14}C Laboratory of CENA/USP, LACUFF (Fluminense Federal University) and at UGAMS (University of Georgia-Center for Applied Isotope Studies). Radiocarbon ages were normalized to a $\delta^{13}C$ of −25‰ VPDB and reported as calibrated years (cal yr BP) (2σ) using CALIB 6.0 (Reimer et al., 2009). The dates are reported in the text as the median of the range of calibrated ages (Table 1).

4. Results

4.1. Radiocarbon date and sedimentation rates

The radiocarbon dates are shown in Table 1 (range since ~8050 cal yr BP) and no age inversions were observed. The sedimentation rates were based on the ratio between the depth intervals (mm) and the time range. The calculated sedimentation rates are 1.5 mm/yr (5.50–4.35 m), 16 mm/yr (4.35–3.45 m), 15 mm/yr (3.45–1.45 m), 0.2 mm/yr (1.45–0.72 m) and 0.2 mm/yr (0.72–0 m). Although the rates are nonlinear between the dated points, they are same magnitude order with the vertical accretion range of 0.1 to 10 mm/yr of mangrove forests reported by other authors (e.g. Behling et al., 2004; Bird, 1980; Cahoon and Lynch, 1997; Cohen et al., 2005a, 2008, 2009; Guimarães et al., 2010; Spenceley, 1982; Vedel et al., 2006).

4.2. Facies, pollen description and isotope values from sediment core

The sediment is composed mostly of greenish gray or dark brown sandy silt with grain size fining upward. The sediment facies are characterized by massive mud, parallel laminated mud, cross stratified sand, parallel-laminated sand, lenticular and heterolithic mud/sand, with peat present near the surface (Figs. 3 and 4). The texture, grain size, sedimentary structures and pollen content, complemented with isotopic and geochemical data ($\delta^{13}C$, $\delta^{15}N$, TOC, N and C/N), define four facies associations representative of foreshore, lagoon, lake, and herbaceous plain environments (Table 2).

4.2.1. Facies association A (foreshore)

Facies association A occurs in the base of the sediment core until ~8050 cal yr BP (Fig. 4). It consists mainly of fine to medium-grained sands which are poorly selected, sand cross-stratified (facies Sc) and parallel-laminated sand (facies Sp), with locally rippled sand and cross-lamination. Shell fragments are present.

The pollen and spore analysis revealed three ecological groups; herbs, mangroves, and trees and shrubs (Fig. 4). The first pollen zone (A) is characterized mainly by a herbaceous pollen represented by Poaceae (~80%), Asteraceae (~18%) and Amaranthaceae (~2%). The mangrove pollen presents a small fraction represented by *Rhizophora* (~8%). Trees and shrubs are generally represented by Euphorbiaceae (~6%) and Rubiaceae (~3%) (Fig. 5).

4.2.2. Facies association B (lagoon)

This facies association corresponds to the depth interval from 5.5 m (~8050 cal yr BP) to 1.5 m (~7115 cal yr BP). These deposits consist of massive mud (facies Mm), which are interbedded with heterolithic mud and sand deposits (facies Hm), lenticular heterolithic muddy silt (facies Hl), parallel-laminated sand (facies Sp) and flaser or wavy heterolithic deposit (facies Hf). Cross lamination is present at 2.1 m and convoluted laminations are present between ~3.5 and 3.75 m. Shell fragments and dwelling structures produced by the benthic fauna are also visible (Fig. 4).

The pollen assembly is characterized by five ecological groups (Figs. 4 and 5), defined by the presence of herbs such as Poaceae (30–80%), Cyperaceae (3–30%), Asteraceae (2–5%), *Borreria* (1–5%), Malvaceae (1–4%), *Smilax* (1–3%), Amaranthaceae (1–3%) and *Polygonum* (~1%). Within this facies association mangrove pollen represented by *Rhizophora* (4–30%) and *Avicennia* (1–3%) is also observed. Tree and shrub species are present as Euphorbiaceae (2–8%), Fabaceae (2–7%), *Mimosa* (1–6%), Rubiaceae (1–5%) and Myrtaceae, Malpighiaceae, Sapindaceae, Meliaceae, and *Podocarpus* with less than 4%, respectively. The Arecaceae occurs between 1–5%, while aquatic species are represented by *Typha* (~2%).

The $\delta^{13}C$ values exhibit a depleted trend from −15 to −27‰ (mean = −20‰) between 5.5 and 1.35 m. The $\delta^{15}N$ record shows stable values between 3.6 and 7.0‰ (mean = 5.3‰). The TOC and N results were also relatively stable between 1.77 to 5.20% (mean = 3.48%) and 0.03 to 0.11% (mean = 0.07%), respectively. The C/N values showed considerable variation between 30 and 60 (mean = 40).

4.2.3. Facies association C (lake)

Facies association C was identified from 1.5 (~7115 cal yr BP) to 0.8 m (~3274 cal yr BP). The grain size of this facies ranges between sandy silt and silty sand, and is poorly sorted, with heterolithic mud/sand (facies Hm) and parallel laminated mud (facies Mp) along with roots, root marks and dwelling structures produced by benthic fauna (Fig. 4).

The pollen record is marked by the shrinkage and eventual disappearance of mangroves, which was mainly constituted by *Rhizophora* (3–15%) and *Avicennia* (1–2%). The other four ecological groups were stable, such as herbs represented by Cyperaceae (25–55%), Poaceae (15–40%), Araceae (5–8%), Amaranthaceae (2–7%), Malvaceae (2–6%), *Borreria* (2–5%) and *Smilax* (1–3%). The tree and shrub section of this facies is represented by *Alchornea* (2–6%), Anacardiaceae (2–5%), Fabaceae (2–4%), Euphorbiaceae (1–4%), *Mimosa* (1–4%), Moraceae (2–3%), Rubiaceae

Table 1
Sediment samples selected for radiocarbon dating and results from LI-32 core (coastal plain of the Doce River) with material, depth, $\delta^{13}C$, ^{14}C conventional and calibrated ages (using CALIB 6.0; Reimer et al., 2009).

Cody site and laboratory number	Depth (m)	Material	Ages (^{14}C yr BP, 1σ)	Ages (cal yr BP, 2σ deviation)	Median of age range (cal yr BP)	Sedimentation rates
LACUFF13019	0.67–0.72	Bulk sed.	2877 ± 79	3246–2840	3043	0.2 mm/yr
LACUFF12039	1.40–1.45	Bulk sed.	6237 ± 66	7278–6955	7116	0.2 mm/yr
UGAMS11695	3.40–3.45	Bulk sed.	6330 ± 30	7318–7172	7245	15.0 mm/yr
UGAMS11694	4.30–4.35	Bulk sed.	6380 ± 30	7339–7259	7300	16.0 mm/yr
LACUFF12040	5.45–5.50	Bulk sed.	7186 ± 54	8161–7933	8047	1.50 mm/yr

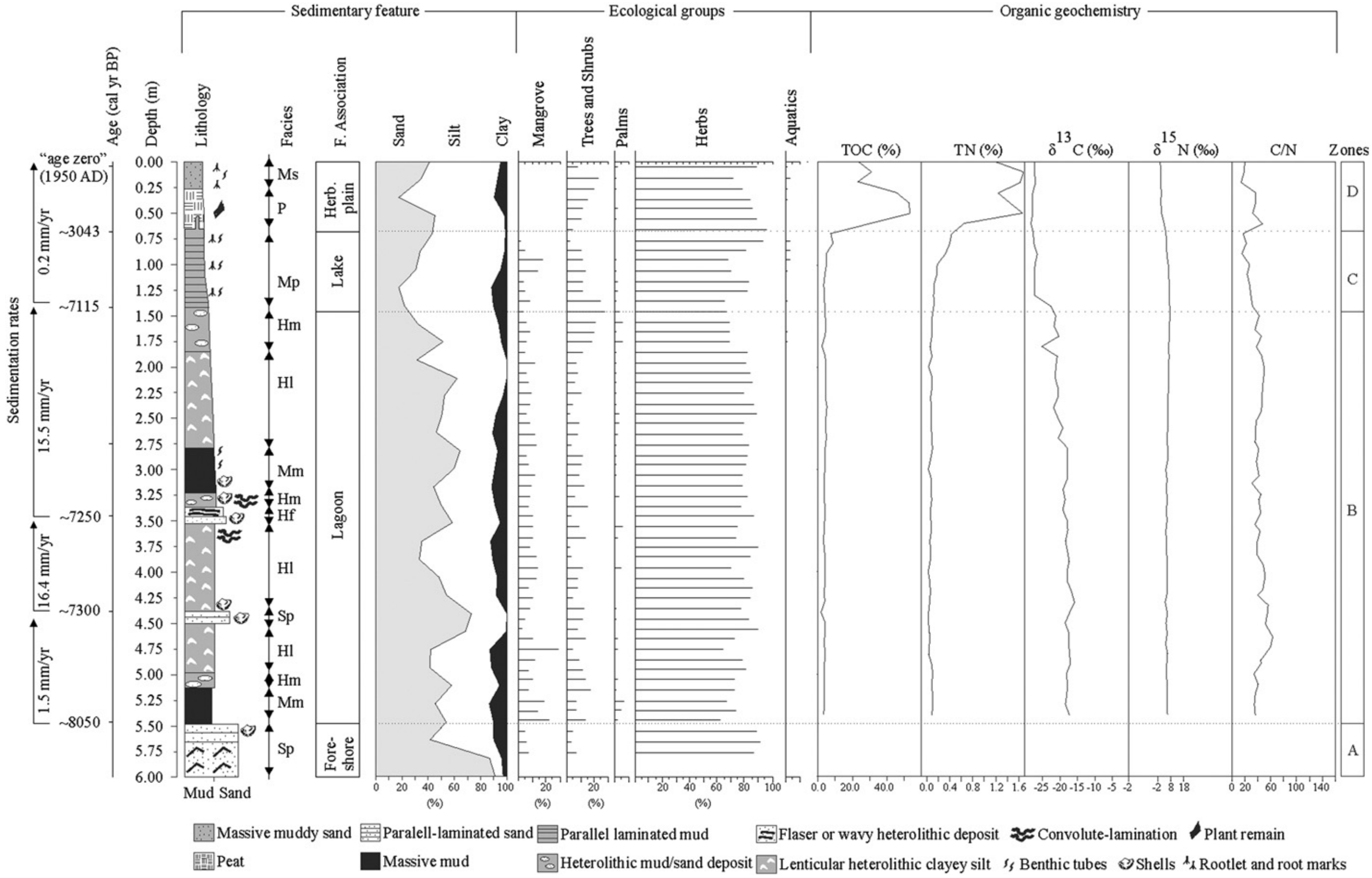

Fig. 4. Summary results for sediment core (LI-32): variation as a function of core depth showing chronological and lithological profile with sedimentary features and facies, pollen analysis with ecological groups, organic geochemical variables and characteristics of organic matter influence. Pollen data are presented in pollen diagrams as percentages of the total pollen sum.

(2–3%), Myrtaceae (~2%), Sapotaceae (~2%), Meliaceae (2%) and Melastomataceae/Combretaceae (1%). The Palm (2–5%) and aquatic pollen groups are represented by *Potamogeton* (1–3%) and *Typha* (~2%) (Fig. 5).

The isotope and elemental data showed different results relative to facies association B, where the $\delta^{13}C$ values exhibit relatively depleted values between −28 and −23‰ (mean = −26‰). The $\delta^{15}N$ values range between 4.5 and 7.2‰ (mean = 5.9‰). The C/N values decrease from 32 to 15 (mean = 23).

4.2.4. Facies association D (herbaceous plain)

The herbaceous plain facies begins at a depth of 0.7 m and continues to the surface. Probably, it was developed during the late-Holocene. These deposits are represented by peat and sandy silt sediments (facies Ms), poorly sorted, with plant debris and evidence of bioturbation (Fig. 4).

The pollen assemblages of this association correspond to zone D, which is composed of four ecological groups (Figs. 4 and 5), and the mangrove group was not present. This zone is characterized by pollen from herbs, trees and shrubs, palms and some aquatics. The herbaceous pollen is represented by Cyperaceae (10–35%), Poaceae (20–30%), Araceae (15–25%), *Smilax* (2–10%), Malvaceae (3–7%) and *Borreria* (2–4%), followed by Amaranthaceae, *Apium*, Asteraceae, *Begonia*, *Coccocypselum*/*Declieuxia*, Convovulaceae, *Polygonum*, *Sauvagesia* and *Xyris* in percentages below 3%. The tree and shrub pollen is represented mainly by *Mimosa* (2–6%), Anacardiaceae (2–6%), Rubiaceae (2–5%), Malpighiaceae (2–4%), *Alchornea* (2–3%) and Fabaceae (1–2%), followed by *Anadenanthera*, Melastomataceae/Combretaceae, Meliaceae and Mytaceae at around 1–2%, respectively. The palm and aquatic pollen were below 2%, colonized by Arecaceae, *Hydrocleis*, *Typha* and *Utricularia*.

The sediment $\delta^{13}C$ values ranged between −28 and −26‰ (mean = −27‰). The range for $\delta^{15}N$ values was between −0.1 and 7‰. The C/N ratio varies between 47 and 16 (mean = 29).

5. Interpretation and discussion

The data suggest two phases of wetland development: (i) tidal flat colonized by mangroves in the margin of the lagoon, where flow energy oscillated. In addition, the geochemical data showed organic matter was influenced by C_4 plants between ~8050 and ~7115 cal yr BP. The phase (ii) was characterized by mangrove extinctions, with an increased influence of C_3 plants and freshwater/estuarine dissolved organic matter, which occurred in the lake and, then the development of a herbaceous plain, probably, during the late-Holocene (Fig. 7).

5.1. Early Holocene: foreshore to lagoon

The foreshore to lagoon phase was initially marked by a foreshore facies association which exhibits shell fragments in cross-stratified sand and parallel-laminated sand (Fig. 4), which record the action of relatively weak currents shaping the bedform. These currents induced the migration of small sand ripples (Reineck and Singh, 1980) between 6 and 5.60 m depth. The ecological record for this region is characterized by mangrove development associated with herbs trees and shrubs (Figs. 5 and 7). The lagoon facies is represented by massive mud, heterolithic mud/sand, lenticular heterolithic muddy silt, parallel-laminated sand, and flaser or wavy heterolithic deposits and cross-laminations. This assemblage of structures may indicate tidal influence. During this period, the tidal flat in the margin of the lagoon was occupied by mangroves, herbs, palms, trees and shrubs

Table 2
Summary of facies association with sedimentary characteristics, pollen groups and geochemical data.

Facies association	Facies description	Pollen predominance	Geochemical data	Interpretation
A	Fine to medium-grained, parallel-laminated sand (facies Sp) and cross-stratified (facies Sc). Greenish gray sand with shells and poorly sorted.	Herbs, mangrove, trees and shrubs		Foreshore
B	Massive mud (facies Mm) greenish gray, with many roots and root marks. Lenticular to streaky (facies Hl), heterolithic mud with sand deposit (facies Hm). Silty sand and sandy silt, fine to medium-grained poorly sorted and locally flaser (facies Hf) with parallel-laminated sand (facies Sp) and with also massive sand, shells and convolute lamination.	Herbs, mangrove, trees and shrubs	$\delta^{13}C = -27$ to -15‰ $\delta^{15}N = +3.6$ to $+7$‰ TOC = 1.7 to 5.2% C/N = 30 to 60	Lagoon
C	Parallel-laminated mud (facies Mp), yellowish brown, with many roots and root marks and dwelling structures and sandy silt.	Herbs, trees, shrubs and mangrove	$\delta^{13}C = -28$ to -23‰ $\delta^{15}N = +4.5$ to $+7$‰ TOC = 3.4 to 8.7% C/N = 15 to 32	Lake
D	Plastic, massive mud and some sandy silt, gray to dark gray and green, with many roots and root marks (facies Ms) and peat deposit (P).	Herbs, trees and shrubs	$\delta^{13}C = -28$ to -26‰ $\delta^{15}N = -0.14$ to $+7$‰ TOC = 7.4 to 53% C/N = 16 to 47	Herbaceous plain

(Fig. 7). Also during this time, the development of the mangrove was largely represented by *Rhizophora* (4–30%), which is associated with trees and shrubs (2–25%), and may have contributed to the upward decrease of $\delta^{13}C$ values from −15‰ to −23‰. It may represent a mixture of C_3, C_4 plants and aquatic organic matter, as indicated by the binary diagram between the $\delta^{13}C$ and C/N rate (Fig. 6). The C_4 plants may be sourced from marine herbs, which have lower $\delta^{13}C$ values (between −17‰ and −9‰, Boutton, 1996). The $\delta^{15}N$ values (mean = 5.2‰) suggest a mixture of terrestrial plants and aquatic organic matter (~5.0‰, Sukigara and Saino, 2005).

5.2. Middle–late Holocene: lagoon/lake transition to herbaceous flat

The transition from a lagoon system to lake/herbaceous flat occurred after 7115 cal yr BP. This environment is marked by increased influence of C_3 plants. The sediment is composed of sandy silt, parallel-laminated mud and some benthic tubes, roots, and root marks, which indicate stagnant conditions. In this phase the mangrove ecosystem became extinct at the study site. The disruption of the mangrove ecosystem during this period indicates unfavorable conditions for mangrove development, which may have been due to decreased pore water salinity. This salinity decrease would have allowed the colonization of herbs, trees, shrubs, palms, and aquatic vegetation in the study site. The $\delta^{13}C$ values from −23‰ to −28‰, indicate an increased influence of C_3 plants (−32‰ to −21‰; Deines, 1980). The relationship between $\delta^{13}C$ and C/N values indicate a mixture of continental and aquatic organic matter, which was dominantly composed of C_3 plants. The presence of aquatic material (Fig. 5) indicates a lacustrine environment. The accumulation of mud and organic matter into the lake led to the filling of lake depressions and expansion of a herbaceous plain during the late-Holocene. During this time the vegetation was characterized mainly by herbs, trees, and shrubs with distinctive isotopic signals and C/N values from C_3 plants (Fig. 6). The $\delta^{15}N$ values exhibit a decreasing trend from 4.3‰ to −0.1‰ in sediments close to the surface (0.7–0 m), suggesting an increased amount of terrestrial organic matter ($\delta^{15}N$ ~ 1‰, Peterson and Howarth, 1987; Fellerhoff et al., 2003). Normally aquatic plants take up dissolved inorganic nitrogen, which is isotopically enriched in ^{15}N by 7‰ to 10‰ relative to atmospheric N (0‰), and thus terrestrial plants that use N_2 derived from the atmosphere have $\delta^{15}N$ values ranging from 0‰ to 2‰ (Meyers, 2003). The C/N ratio (mean = 29) also indicates organic matter from vascular plants (>12 vascular plants, Meyers, 1994; Tyson, 1995). The binary diagram of $\delta^{13}C$ vs. C/N ratio reveals the contribution of C_3 terrestrial plants (Fig. 6).

5.3. Holocene sea-level changes, climate and vegetation dynamics

The data suggest mangrove vegetation and C_4 plants on a tidal flat surrounding a lagoon between ~8050 and ~7115 cal yr BP. This phase was followed by a decrease in mangrove habitat and an expansion of C_3 terrestrial plants represented by herbs, trees and shrubs. These results suggest a transition from marine to freshwater influence, likely

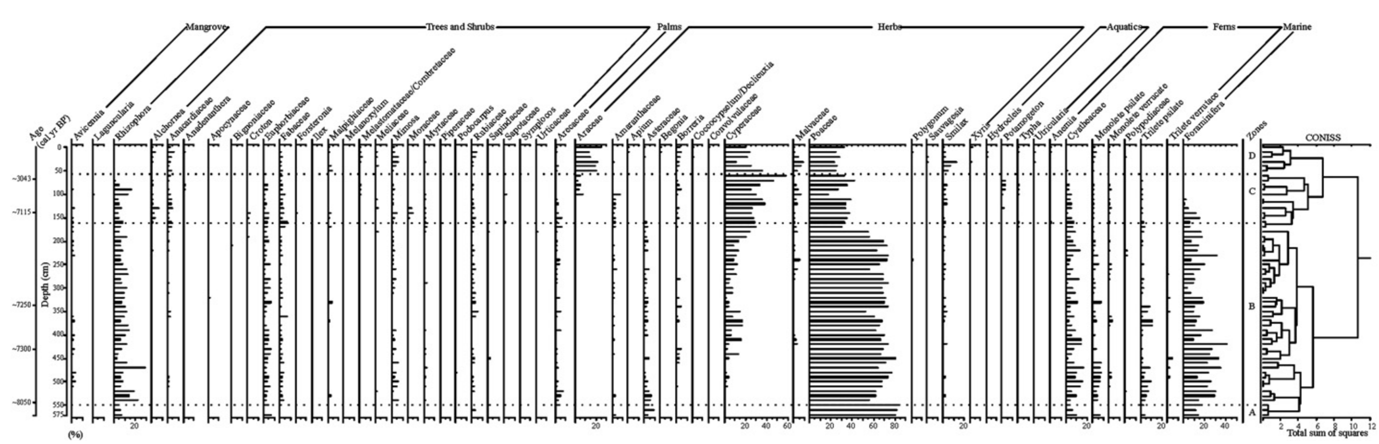

Fig. 5. Pollen diagram record with percentages of the most frequent pollen taxa, sample age, zones and cluster analysis.

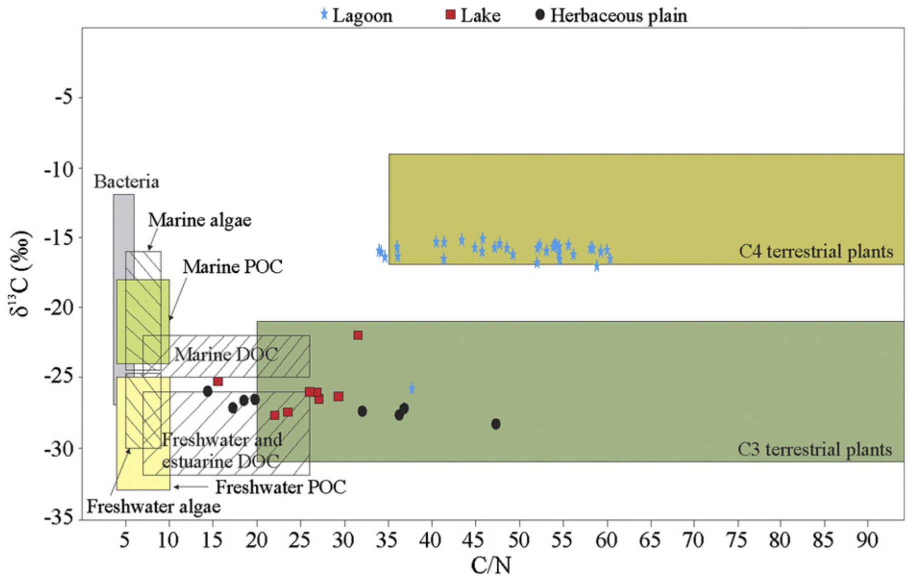

Fig. 6. Diagram illustrating the relationship between $\delta^{13}C$ and C/N ratio for the different sedimentary facies (foreshore, lagoon, lake and herbaceous plain), with interpretation according to data presented by Lamb et al. (2006); Meyers (2003) and Wilson et al. (2005) showing C_4 plants with marine/brackish water influence and C_3 plants with freshwater influence.

due to the combined action of RSL fall and sedimentary supply during the mid- and late-Holocene.

During the lagoon phase (~8050 and ~7115 cal yr BP) the sedimentation rates (16.4–15.5 mm/yr) were higher than the lacustrine and herbaceous plain phase (0.2 mm/yr) over the past ~7115 cal yr BP (Fig. 4). It may be related to the post-glacial sea-level rise in the early-Holocene, when more space was created to accommodate new sediments (Fig. 8), while during the mid- and late-Holocene occurred RSL fall with the decrease in accommodation space.

Changes in the RSL, sedimentary supply and river discharge during the Holocene are important processes that influenced not only the relative position of the shoreline, but also the characteristics of coastal stratigraphic systems and vegetation dynamics (Buso Jr., 2010; Cohen et al., 2005a,b, 2012; França et al., 2012; Guimarães et al., 2012; Scheel-Ybert, 2000; Smith et al., 2012) (Fig. 8). Probably, the RSL changes along the Brazilian littoral must be the main driving force controlling the mangrove dynamics, while the sedimentary supply, mainly in the southern Brazil, and tidal water salinity, mainly in the northern Brazil, may be considered as secondary causes (Cohen et al., 2012).

Considering the RSL changes, references to the highstand along eastern coast of Brazil can be found in several publications, including Suguio et al. (1985), Dominguez et al. (1990), Angulo and Suguio (1995), Angulo and Lessa (1997), Angulo et al. (1999), Souza et al. (2001), Bezerra et al. (2003), Martin et al. (2003) and Angulo et al. (2006).

The RSL curve during the mid- to late-Holocene, along northeastern Brazil, was reconstructed by Martin et al. (2003), who showed that RSL exceeded the present level around 7700 cal yr BP and 5600 cal yr BP, followed by fast regression between 5300 and 4200 cal yr BP when the RSL may have been below the current level (Fig. 8). A fast rise occurred again approximately 3700 cal yr BP with a maximum of 3.5 $\pm$ 0.5 m above the present RSL, followed by a steady and slow decrease between 3500 and 2800 cal yr BP. At 2800 cal yr BP, sea level fell quickly, falling below the current level by 2600 cal yr BP. About 2300 cal yr BP, RSL began to rise, reaching 2.3 $\pm$ 0.5 m above the present level by 2100 cal yr BP. After 2100 cal yr BP RSL fell steadily to its current position (Fig. 8). Other studies performed along the eastern and southeastern Brazilian coast also showed the existence of three paleo-sea-levels higher than the present (Martin et al., 1987, 1996; Suguio et al., 1982, 1985). However, Angulo et al. (2006) proposed a mid-Holocene RSL maximum above present RSL and subsequent fall to the present time, without subsequent oscillation (Fig. 8).

Along the coast of southeastern Brazil, higher RSL led to the formation of numerous lagoons (Sallun et al., 2012), and estuaries as observed in a recent study developed in the region (Buso Jr., 2010). This information is relevant to our study because between >8050 and ~7115 cal yr BP the sedimentary features reveal a facies association typically of foreshore and lagoon systems with mangrove, likely a consequence of high RSL during this time (Fig. 8). During the mid- and late-Holocene there was a retraction of mangrove and expansion of herbaceous vegetation, trees and shrubs followed by an increase in the contribution of freshwater organic matter. During this phase, a lake was developed following a regressive phase. During this period C_3 plants became the dominant vegetation in the study region. The flow of sediments led to siltation and infilling of the lacustrine setting, causing the expansion of the herbaceous plain ecosystem seen today (Fig. 7).

6. Conclusion

This study indicates the presence of a lagoon system surrounded by a tidal plain colonized by mangroves, and its sedimentary organic matter sourced from C_4 plants, between ~8050 and ~7115 cal yr BP. However, during the mid- and late-Holocene the mangroves shrank and freshwater vegetation expanded (C_3 plants), probably, due to the combined action of RSL fall and sedimentary supply. During this time, the development of a lacustrine environment was followed by the colonization of herbs, trees and shrubs. The continuous infilling of sediment into the lake allowed the expansion of a herbaceous plain, as seen today. The geomorphologic and vegetation evolution is in agreement with the mid-Holocene RSL maximum above present RSL and subsequent fall to the present time, as proposed by Angulo et al. (2006).

Acknowledgments

We would like to thank the members of the Laboratory of Costal Dynamic (LADIC-UFPA), Center for Nuclear Energy in Agriculture (CENA/USP), and Climate System Research Center (CSCR/UMass), and the students from the Laboratory of Chemical-Oceanography and Vale Natural Reserve, Linhares, ES, for their support. This study was financed by FAPESP (03615-5/2007 and 00995-7/2011) and CNPq (Universal 470210/2012-5). The first author received a scholarship from CNPq (Process 202598/2011-0). The authors would also like to thank Raymond S. Bradley and Gregory de Wet (CSRC/UMass) for the English revision of this paper.

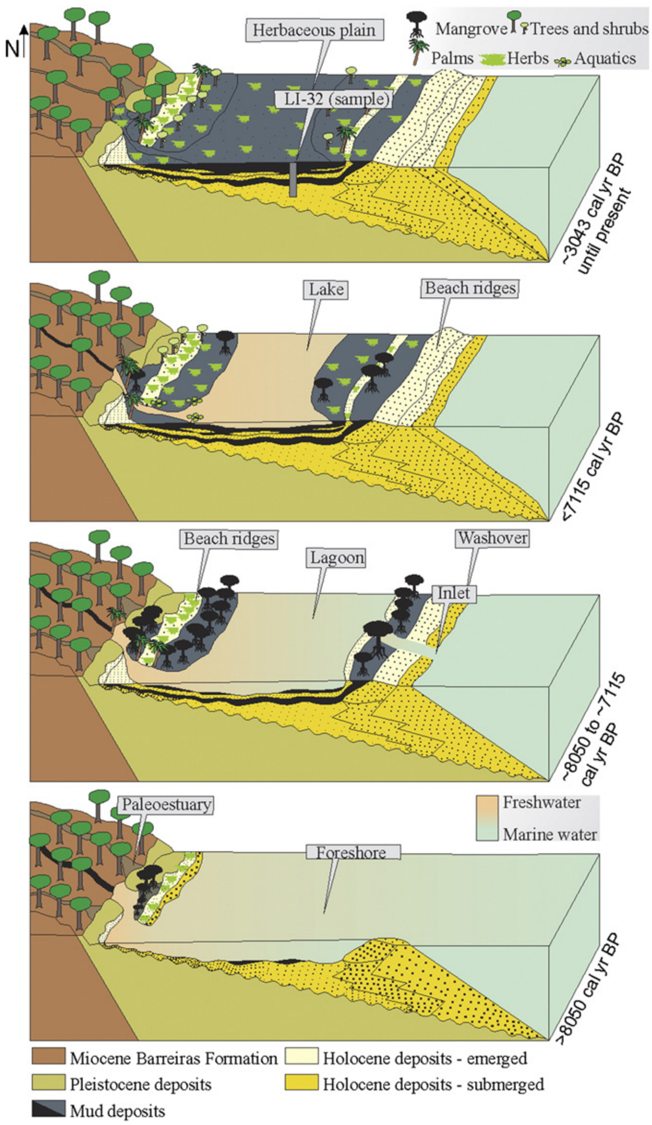

Fig. 7. Model of the geomorphology and vegetation development with successive phases of sediment accumulation according to relative sea-level changes during the Holocene.

References

Absy, M.L., 1975. Polen e esporos do Quaternário de Santos (Brasil). Hoehnea 5, 1–26.

Alongi, D.M., 2008. Mangrove forests: resilience, protection from tsunamis, and responses to global climate change. Estuarine, Coastal and Shelf Science 76, 1–13.

Amaral, P.G.C., Ledru, M.P., Branco, F.R., Giannini, P.C.F., 2006. Late Holocene development of a mangrove ecosystem in southeastern Brazil (Itanhaém, state of São Paulo). Palaeogeography, Palaeoclimatology, Palaeoecology 241, 608–620.

Amaral, P.G.C., Giannini, P.C.F., Sylvestre, F., Pessenda, L.C.R., 2012. Paleoenviromental reconstruction of a Late Quaternary lagoon system in southern Brazil (Jaguaruna Region, Santa Catarina State) based on multi-proxy analysis. Journal of Quaternary Science 27, 181–191.

Andersen, S.T., 1967. Tree-pollen rain in a mixed deciduous forest in south Jutland (Denmark). Review of Palaeobotany and Palynology 3, 267–275.

Angulo, R.J., Lessa, G.C., 1997. The Brazilian sea-level curves: a critical review with emphasis on the curves from the Paranaguá and Cananéia regions. Marine Geology 140, 141–166.

Angulo, R.J., Suguio, K., 1995. Re-evaluation of the Holocene sea-level maxima for the State of Paraná, Brazil. Palaeogeography, Palaeoclimatology, Palaeoecology 113, 385–393.

Angulo, R.J., Giannini, P.C.F., Suguio, K., Pessenda, L.C.R., 1999. Relative sea-level changes in the last 5500 years in southern Brazil (Laguna–Imbituba region, Santa Catarina State) based on vermitid ^{14}C ages. Marine Geology 159, 323–339.

Angulo, R.J., Lessa, G.C., Souza, M.C., 2006. A critical review of mid- to late-Holocene sea-level fluctuations on the eastern Brazilian coastline. Quaternary Science Reviews 25, 486–506.

Asmus, H.E., Gomes, J.B., Pereira, A.C.B., 1971. Integração geológica regional da bacia do Espírito Santo. in: Anais do XXV Congresso Brasileiro de Geologia (SBG). São Paulo, SP, Brasil. pp. 235–254.

Arai, M., 2006. A grande elevação eustática do Mioceno e sua influência na origem do Grupo Barreiras. Geologia USP Série Científica 6, 1–6.

Behling, H., Cohen, M.C.L., Lara, R.J., 2001. Studies on Holocene mangrove ecosystem dynamics of the Bragança Peninsula in north-eastern Pará, Brazil. Palaeogeography, Palaeoclimatology, Palaeoecology 167, 225–242.

Behling, H., Cohen, M.C.L., Lara, R.J., 2004. Late Holocene mangrove dynamics of the Marajó Island in northern Brazil. Vegetation History and Archaeobotany 13, 73–80.

Bernini, E., Silva, M.A.B., Carmo, T.M.S., Cuzzuol, G.R.F., 2006. Composição química do sedimento e de folhas das espécies do manguezal do estuário do Rio São Mateus, Espírito Santo, Brasil. Revista Brasileira de Botânica 29, 689–699.

Bezerra, F.H.R., Barreto, A.M.F., Suguio, K., 2003. Holocene sea-level history on the Rio Grande do Norte State coast, Brazil. Marine Geology 196, 73–89.

Bird, E.C.F., 1980. Mangroves and coastal morphology. The Victorian Naturalist 97, 48–58.

Bittencourt, A.C.S.P., Martin, L., Vilas-Boas, G.S., Flexor, J.M., 1979. Quaternary marine formations of the coast of the State of Bahia, Brazil. Coastal Evolution in the Quaternary 232–253.

Bittencourt, A.C.S.P., Dominguez, J.M.L., Martin, L., Silva, I.R., De-Medeiros, K.O.P., 2007. Past and current sediment dispersion pattern estimates through numerical modeling of wave climate: an example of the Holocene delta of the Doce River, Espírito Santo, Brazil. Anais da Academia Brasileira de Ciências 79, 333–341.

Blasco, F., Saenger, P., Janodet, E., 1996. Mangrove as indicators of coastal change. Catena 27, 167–178.

Boutton, T.W., 1996. Stable carbon isotope ratios of soil organic matter and their use as indicators of vegetation and climate change. In: Boutton, T.W., Yamasaki, S.I. (Eds.), Mass Spectrometry of Soils. Marcel Dekker, New York, NY.

Buso Junior, A.A., 2010. Dinâmica ambiental holocênica (vegetação, clima e nível relativo marinho) baseada em estudos interdisciplinares de alta resolução, no litoral norte do estado do Espírito Santo. Universidade de São Paulo, Programa de Pós-Graduação em Ciências, Piracicaba-SP 190 (Dissertação de Mestrado).

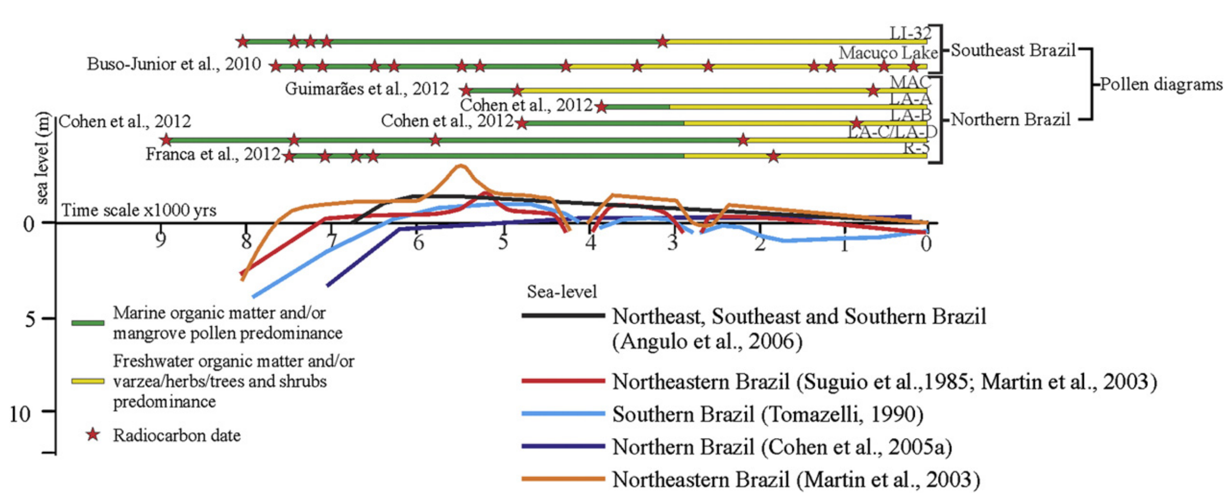

Fig. 8. RSL curves of the eastern Brazilian coast during the Holocene with comparative pollen diagrams from northern and southeast Brazil coastline.

Buso Junior, A.A., Pessenda, L.C.R., de Oliveira, P.E., Giannini, P.C.F., Cohen, M.C.L., Volkmer-Ribeiro, C., Oliveira, S.M.B., Favaro, D.I.T., Rossetti, D.F., Lorente, F.L., Borotti Filho, M.A., Schiavo, J.A., Bendassolli, J.A., Siqueira, G.S., 2013. From an estuary to a freshwater lake: a paleo-estuary evolution in the context of Holocene sea-level fluctuations, southeastern Brazil. Radiocarbon (in press).

Cahoon, D.R., Lynch, J.C., 1997. Vertical accretion and shallow subsidence in a mangrove forest of southwestern Florida, U.S.A. Mangroves and Salt Marshes 3, 173–186.

Carvalho, L.M.V., Jones, C., Liebmann, B., 2004. The South Atlantic Convergence Zone: intensity, form, persistence, and relationships with intraseasonal to interannual activity and extreme rainfall. Journal of Climate 17, 88–108.

Cohen, M.C.L., 2003. Past and Current Mangrove Dynamics on the Bragança península, Northern Brasil. Universität Bremen. Zentrum für Marine Tropenökologie, Bremen 110 (Dissertation (Doktorgrades) Universität Bremen).

Cohen, M.C.L., Lara, R.J., 2003. Temporal changes of mangrove vegetation boundaries in Amazonia: application of GIS and remote sensing techniques. Wetlands Ecology and Management 11, 223–231.

Cohen, M.C.L., Lara, R.J., Szlafsztein, C.F., Dittmar, T., 2004. Mangrove inundation and nutrient dynamics under a GIS perspective. Wetlands Ecology and Management 12, 81–86.

Cohen, M.C.L., Behling, H., Lara, R.J., 2005a. Amazonian mangrove dynamics during the last millennium: the relative sea-level and the little Ice Age. Review of Palaeobotany and Palynology 136, 93–108.

Cohen, M.C.L., Souza Filho, P.W., Lara, R.L., Behling, H., Angulo, R., 2005b. A model of Holocene mangrove development and relative sea-level changes on the Bragança Peninsula (northern Brazil). Wetlands Ecology and Management 13, 433–443.

Cohen, M.C.L., Lara, R.J., Smith, C.B., Angélica, R.S., Dias, B.S., Pequeno, T., 2008. Wetland dynamics of Marajó Island, northern Brazil, during the last 1000 years. Catena 76, 70–77.

Cohen, M.C.L., Lara, R.J., Smith, C.B., Matos, H.R.S., Vedel, V., 2009. Impact of sea-level and climatic changes on the Amazon coastal wetlands during the late Holocene. Vegetation History and Archaeobotany 18, 425–439.

Cohen, M.C.L., Pessenda, L.C.R., Behling, H., Rossetti, D.F., França, M.C., Guimarães, J.T.F., Friaes, Y.S., Smith, C.B., 2012. Holocene palaeoenvironmental history of the Amazonian mangrove belt. Quaternary Science Reviews 55, 50–58.

Colinvaux, P., De Oliveira, P.E., Patiño, J.E.M., 1999. Amazon Pollen Manual and Atlas. Harwood Academic Publishers, Dordrecht (332 pp.).

Davis, M.B., 2000. Palynology after Y2K—understanding the source area of pollen in sediments. Annual Review of Earth and Planetary Sciences 28, 1–18.

Deines, P., 1980. The isotopic composition of reduced organic carbon. In: Fritz, P., Fontes, J.C. (Eds.), Handbook of Environmental Isotope Geochemistry. The Terrestrial Environments, vol. 1. Elsevier, Amsterdam, pp. 329–406.

Dominguez, J.M.L., Bittencourt, A.C.S.P., Leão, Z.M.A.N., Azevedo, A.E.G., 1990. Geologia do Quaternário costeiro do estado de Pernambuco. Revista Brasileira de Geociências 20, 208–215.

Dominguez, J.M.L., Bittencourt, A.C.S.P., Martin, L., 1992. Controls on Quaternary coastal evolution of the east-northeastern coast of Brazil: roles of sea-level history, trade winds and climate. Sedimentary Geology 80, 213–232.

Dominguez, J.M.L., Andrade, A.C.S., Almeida, A.B., Bittencourt, A.C.S.P., 2009. The Holocene barrier strandplains of the State of Bahia. In: Dillenburg, S., Hesp, P. (Eds.), Geology and Geomorphology of Holocene Coastal Barriers of Brazil. Springer, Berlin, Germany, pp. 253–288.

Ellison, J.C., 2005. Holocene palynology and sea-level change in two estuaries in Southern Irian Jaya. Palaeogeography, Palaeoclimatology, Palaeoecology 220, 291–309.

Engelhart, S.E., Horton, B.P., Roberts, D.H., Bryant, C.L., Corbett, D.R., 2007. Mangrove pollen of Indonesia and its suitability as a sea-level indicator. Marine Geology 242, 65–81.

Faegri, K., Iversen, J., 1989. Textbook of Pollen Analysis, 4th ed. John Wiley and Sons, Chichester 328.

Fellerhoff, C., Voss, M., Wantzen, K.M., 2003. Stable carbon and nitrogen isotope signatures of decomposing tropical macrophytes. Aquatic Ecology 37, 361–375.

França, M.C., 2010. Mudanças na vegetação do litoral Leste da Ilha de Marajó durante o Holoceno Superior. Dissertação de Mestrado Instituto de Geociências, Universidade Federal do Pará (111 pp.).

França, M.C., Francisquini, M.I., Cohen, M.C.L., Pessenda, L.C.R., Rossetti, D.F., Guimarães, J.T.F., Smith, C.B., 2012. The last mangroves of Marajó Island — Eastern Amazon: impact of climate and/or relative sea-level changes. Review of Paleobotany and Palynology 187, 50–65.

Fujimoto, K., Miyagi, T., Kikuchi, T., Kawana, T., 1996. Mangrove habitat formation and response to Holocene sea-level changes on Kosrae Island, Micronesia. Mangroves and Salt Marshes 1, 47–57.

Giannini, P.C.F., Sawakuchi, A.O., Martinho, C.T., Tatumi, S.H., 2007. Eolian depositional episodes controlled by Late Quaternary relative sea level changes on the Imbituba Laguna coast (southern Brazil). Marine Geology 237, 143–168.

Goh, K.M., 2006. Removal of contaminants to improve the reliability of radiocarbon dates of peats. Journal of Soil Science 29, 340–349.

Grimm, E.C., 1987. CONISS: a FORTRAN 77 program for stratigraphically constrained cluster analysis by the method of the incremental sum of squares. Computer and Geosciences 13, 13–35.

Grimm, E.C., 1990. TILIA and TILIAGRAPH: PC spreadsheet and graphic software for pollen data. INQUA Subcommission on Data-handling MethodsNewsletter 4, 5–7.

Guimarães, J.T.F., Cohen, M.C.L., França, M.C., Lara, R.J., Behling, H., 2010. Model of wetland development of the Amapá coast during the late Holocene. Anais da Academia Brasileira de Ciências 82, 451–465.

Guimarães, J.T.F., Cohen, M.C.L., Pessenda, L.C.R., França, M.C., Smith, C.B., Nogueira, A.C.R., 2012. Mid- and late-Holocene sedimentary process and palaeovegetation changes near the mouth of the Amazon River. The Holocene 22, 359–370.

Guimarães, J.T.F., Cohen, M.C.L., França, M.C., Pessenda, L.R., Behling, H., 2013. Morphological and vegetation changes on tidal flats of the Amazon Coast during the last 5000 cal. yr BP. The Holocene 23, 528–543.

Harper, C.W., 1984. Improved methods of facies sequence analysis, In: Walker, R.G. (Ed.), Facies Models, 2nd ed. Geological Association of Canada, Ontario, Canada, pp. 11–13.

Horton, B.P., Gibbard, P.L., Milne, G.A., Morley, R.J., Purintavaragul, C., Stargardt, J.M., 2005. Holocene sea levels and palaeoenvironments, Malay–Thai Peninsula, Southeast Asia. The Holocene 15, 1199–1213.

Janssen, C.R., 1966. Recent pollen spectra from the deciduous and coniferous deciduous forests of northeastern Minnesota: a study in pollen dispersal. Ecology 47, 804–825.

Janssen, C.R., 1973. Local and regional pollen deposition. In: Birks, H.J.B., West, R.G. (Eds.), Quaternary Plant Ecology. Blackwell, Oxford, UK, pp. 31–42 (326 pp.).

Lamb, A.L., Wilson, G.P., Leng, M.J., 2006. A review of coastal palaeoclimate and relative sea-level reconstructions using $\delta^{13}C$ and C/N ratios in organic material. Earth-Science Reviews 75, 29–57.

Lara, R.J., Cohen, M.C.L., 2009. Palaeolimnological studies and ancient maps confirm secular climate fluctuations in Amazonia. Climatic Change 94, 399–408.

Lara, R., Szlafsztein, C., Cohen, M.C.L., Berger, U., Marion, G., 2002. Implications of mangrove dynamics for private land use in Bragança, North Brazil: a case study. Journal of Coastal Conservation 8, 97–102.

Lugo, A.E., Snedaker, S.C., 1974. The ecology of mangroves. Annual Review of Ecology and Systematics 5, 39–64.

Markgraf, V., D'Antoni, H.L., 1978. Pollen Flora of Argentina. University of Arizona Press, Tucson.

Martin, L., Suguio, K., 1992. Variation of coastal dynamics during the last 7000 years recorded in beach-ridge plains associated with river mouths: example from the central Brazilian coast. Palaeogeography, Palaeoclimatology, Palaeoecology 99, 119–140.

Martin, L., Suguio, K., Flexor, J.M., 1987. Flutuações do nível relativo do mar no Quaternário e seu papel na sedimentação costeira: Exemplos brasileiros. Simpósio de Ecossistemas da Costa Sul Sudeste Brasileira. , vol. 1. Publicação CIESP, pp. 40–61.

Martin, L., Suguio, K., Flexor, J.M., Dominguez, J.M.L., Bittencourt, A.C.S.P., 1996. Quaternary sea-level history and variation in dynamics along the central Brazil Coast: consequences on coastal plain construction. Anais da Academia Brasileira de Ciências 68, 303–354.

Martin, L., Dominguez, J.M.L., Bittencourt, A.C.S.P., 1998. Climatic control on coastal erosion during a sea-level fall episode. Anais da Academia Brasileira de Ciências 70, 249–266.

Martin, L., Dominguez, J.M.L., Bittencourt, A.C.S.P., 2003. Fluctuating Holocene sea levels is eastern and southeastern Brazil: evidence from a multiple fossil and geometric indicators. Journal of Coastal Research 19, 101–124.

Meyers, P.A., 1994. Preservation of elemental and isotopic source identification of sedimentary organic matter. Chemical Geology 114, 289–302.

Meyers, P.A., 2003. Applications of organic geochemistry to paleolimnological reconstructions: a summary of examples from the Laurentian Great Lakes. Organic Geochemistry 34, 261–289.

Miall, A.D., 1978. Facies types and vertical profile models in braided river deposits: a summary. In: Miall, A.D. (Ed.), Fluvial Sedimentology. Canadian Society of Petroleum Geologists, Calgary, pp. 597–604.

Monacci, N.M., Meier-Gruenhagen, U., Finney, B.P., Behling, H., Wooller, M.J., 2009. Mangrove ecosystem changes during the Holocene at Spanish Lookout Cay, Belize. Palaeogeography, Palaeoclimatology, Palaeoecology 280, 37–46.

Monacci, N.M., Meier-Gruenhagen, U., Finney, B.P., Behling, H., Wooller, M.J., 2011. Paleoecology of mangroves along the Sibun River, Belize. Quaternary Research 76, 220–228.

Munsell Color, 2009. Munsell Soil Color Charts, New Revised Edition. Macbeth Division of Kollmorgen Instruments, New Windsor, NY.

Parkinson, R.W., Delaune, R.D., White, J.R., 1994. Holocene sea-level rise and the fate of mangrove forests within the wider Caribbean region. Journal of Coastal Research 10, 1077–1086.

Peixoto, A.L., Gentry, A., 1990. Diversidade e composição florística da mata de tabuleiros na Reserva Florestal de Linhares (Espírito Santo, Brasil). Revista Brasileira de Botânica 13, 19–25.

Pessenda, L.C.R., Ribeiro, A.S., Gouveia, S.E.M., Aravena, R., Boulet, R., Bendassoli, J.A., 2004. Vegetation dynamics during the late Pleistocene in the Barreirinhas region, Maranhão State, northeastern Brazil, based on carbon isotopes in soil organic mater. Quaternary Research 62, 183–193.

Pessenda, L.C.R., Saia, S.E.M.G., Gouveia, S.E.M., Ledru, M.-P., Siffedine, A., Amaral, P.G.C., Bendassolli, J.A., 2010. Last millennium environmental changes and climate inferences in the Southeastern Atlantic Forest, Brazil. Anais da Academia Brasileira de Ciências 82 (3), 717–729.

Pessenda, L.C.R., Vidotto, E., De Oliveira, P.E., Buso-Jr, A.A., Cohen, M.C.L., Rossetti, D.F., Ricardi-Branco, F., 2012. Late Quaternary vegetation and coastal environmental changes at Ilha do Cardoso mangrove record, southeastern Brazil. Palaeogeography, Palaeoclimatology, Palaeoecology 363–364, 57–68.

Peterson, B.J., Howarth, R.W., 1987. Sulfur, carbon, and nitrogen isotopes used to trace organic matter flow in the salt-marsh estuary of Sapelo Island, Georgia. Limnology and Oceanography 32, 1195–1213.

Reimer, P.J., Baillie, M.G.L., Bard, E., Bayliss, A., Beck, J.W., Blackwell, P.G., Bronk Ramsey, C., Buck, C.E., Burr, G.S., Edwards, R.L., Friedrich, M., Grootes, P.M., Guilderson, T.P., Hajdas, I., Heaton, T.J., Hogg, A.G., Hughen, K.A., Kaiser, K.F., Kromer, B., Mccormac, F.G., Manning, S.W., Reimer, R.W., Richards, D.A., Southon, J.R., Talamo, S., Turney, C.S.M., Van der Plicht, J., Weyhenmeyer, C.E., 2009. IntCal09 and Marine09 radiocarbon age calibration curves, 0–50,000 years cal BP. Radiocarbon 51, 1111–1150.

Reineck, H.E., Singh, I.B., 1980. Depositional Sedimentary Environments with Reference to Terrigenous Clastics, Second edition. Springer-Verlag, Berlin (542 pp.).

Roubik, D.W., Moreno, J.E., 1991. Pollen and spores of Barro Colorado Island. Missouri Botanical Garden Press, St. Louis 270 (Monographs in Systematic Botany, v.36).
Salgado-Labouriau, M.L., 1973. Contribuição à palinologia dos cerrados. Academia Brasileira de Ciências, Rio de Janeiro (273 pp.).
Sallun, A.E.M., Filho, W.S., Suguio, K., Babinski, M., Gioia, S.M.C.L., Harlow, B.A., Duleba, W., Oliveira, P.E., Garcia, V.J., Weber, C.Z., Christofoletti, S.R., Santos, C.S., Medeiros, V.B., Silva, J.B., Santiago-Hussein, M.C., Fernandes, R.S., 2012. Geochemical evidence of the 8.2 ka event and other Holocene environmental changes recorded in paleolagoon sediments southeastern Brazil. Quaternary Research 77, 31–43.
Sanders, C.J., Smoak, J.M., Waters, M.N., Sanders, L.M., Bradini, N., Patchineelam, S.R., 2012. Organic matter content and particle size modifications in mangrove sediments as responses to sea-level rise. Marine Environmental Research 77, 150–155.
Schaeffer-Novelli, Y., Cintrón, G.M., Adaime, R.R., 1990. Variability of mangroves ecosystems along Brazilian coast. Estuaries 13, 204–218.
Schaeffer-Novelli, Y., Cintrón, G., Soares, M.L.G., Tognella-de-Rosa, M.M.P., 2000. Brazilian mangroves. Aquatic Ecosystem Health and Management 3, 561–570.
Scheel-Ybert, R., 2000. Vegetation stability in the Southeastern Brazilian coastal area from 5500 to 1400 ^{14}C yr BP deduced from charcoal analysis. Review of Paleobotany and Palynology 110, 111–138.
Smith, C.B., Cohen, M.C.L., Pessenda, L.C.R., França, M., Guimarães, J.T.F., Rossetti, D.F., 2011. Holocene coastal vegetation changes at the mouth of the Amazon River. Review of Palaeobotany and Palynology 168, 21–30.
Smith, C.B., Cohen, M.C.L., Pessenda, L.C.R., França, M.C., Guimarães, J.T.F., 2012. Holocenic proxies of sedimentary organic matter and the evolution of Lake Arari-Northern Brazil. Catena 90, 26–38.
Soares, M.L.G., Estrada, G.C.D., Fernandez, V., Tognella, M.M.P., 2012. Southern limit of the Western South Atlantic mangroves: assessment of the potential effects of global warming from a biogeographical perspective. Estuarine, Coastal and Shelf Science 101, 44–53.
Souza Filho, P.W.M., Martins, E.S.F., Costa, F.R., 2006. Using mangroves as a geological indicator of coastal changes in the Bragança macrotidal flat, Brazilian Amazon: a remote sensing data approach. Ocean and Coastal Management 49, 462–475.
Souza, M.C., Angulo, R.J., Pessenda, L.C.R., 2001. Evolução paleogeográfica da planície costeira de Itapoá, litoral norte de Santa Catarina. Revista Brasileira de Geociências 31, 223–230.
Spenceley, A.P., 1982. Sedimentation patterns in a mangal on Magnetic Island near Townsville, North Queensland, Australia. Singapore Journal of Tropical Geography 3, 100–107.
Sugita, S., 1994. Pollen representation of vegetation in quaternary sediments: theory and method in patchy vegetation. Journal of Ecology 82, 881–897.
Suguio, K., Martin, L., Dominguez, J.M.L., 1982. Evolução da planície costeira do Rio Doce (ES) durante o Quaternário: influência das flutuações do nível do mar. Atas do IV Simpósio do Quaternário no Brasil, pp. 93–116.
Suguio, K., Martin, L., Bittencourt, A.C.S.P., Dominguez, J.M.L., Flexor, J.M., Azevedo, A.E.G., 1985. Flutuações do Nível do Mar durante o Quaternário Superior ao longo do Litoral Brasileiro e suas Implicações na Sedimentação Costeira. Revista Brasileira de Geociência 15, 273–286.
Sukigara, C., Saino, T., 2005. Temporal variations of $\delta^{13}C$ and $\delta^{15}N$ in organic particles collected by a sediment trap at time-series station off the Tokyo Bay. Continental Shelf Research 25, 1749–1767.
Tyson, R.V., 1995. Sedimentary Organic Matter: Organic Facies and Palynofacies. Chapman and Hall, London (15 pp.).
Vedel, V., Behling, H., Cohen, M.C.L., Lara, R.J., 2006. Holocene mangrove dynamics and sea-level changes in Taperebal, northeastern Pará State, northern Brazil. Vegetation History and Archaeobotany 15, 115–123.
Walker, R.G., 1992. Facies, facies models and modern stratigraphic concepts. In: Walker, R.G., James, N.P. (Eds.), Facies Models — Response to Sea Level Change. Geological Association of Canada, Ontario, Canara, pp. 1–14.
Wentworth, C.K., 1922. A scale of grade and class terms for clastic sediments. Journal of Geology 30, 377–392.
Wilson, G.P., Lamb, A.L., Leng, M.J., Gonzalez, S., Huddart, D., 2005. δ13C and C/N as potential coastal palaeoenvironmental indicators in the Mersey Estuary, UK. Quaternary Science Reviews 24, 2015–2029.
Woodroffe, C.D., 1981. Mangrove swamp stratigraphy and Holocene transgression, Grand Cayman Island, West India. Marine Geology 41, 271–294.
Yulianto, E., Sukapti, W.S., Rahardjo, A.T., Noeradi, D., Siregar, D.A., Suparan, P., Hirakawa, K., 2004. Mangrove shoreline responses to Holocene environmental change, Makassar Strait Indonesia. Review of Palaeobotany and Palynology 131, 251–268.
Yulianto, E., Rahardjo, A.T., Noeradi, D., Siregar, D.A., Hirakawa, K., 2005. A Holocene pollen record of vegetation and coastal environmental changes in the coastal swamp forest at Batulicin, South Kalimantan, Indonesia. Journal of Asian Earth Sciences 25, 1–8.